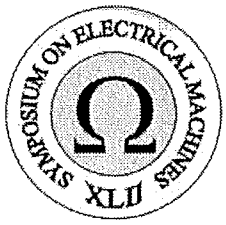

Electromagnetically excited audible noise – evaluation and optimisation of electrical machines by numerical simulation

Christoph SCHLENSOK*, Benedikt SCHMÜLLING*,
Michael VAN DER GIET*, Kay HAMEYER*

* RWTH Aachen University, Institute of Electrical Machines (IEM)
Schinkelstr. 4, D-52056 Aachen, Germany
E-Mail: Christoph.Schlensok@iem.rwth-aachen.de

ABSTRACT

Disturbing vibrations and noise of electrical machines are gaining impact. Therefore, it is necessary to estimate the electromagnetic, structure-dynamical, and acoustic behaviour of the machine during designing and before prototyping. An adequate tool is numerical simulation applying the Finite-Element Method (FEM) and the Boundary-Element Method (BEM) allowing for the structured analysis and evaluation of audible noise also caused by manufacturing tolerances. The methods developed and proved at the Institute of Electrical Machines (IEM) at RWTH Aachen University can be applied to any electromagnetic device in general.

Keywords: FEM, BEM, multi-physics, coupled simulation, acoustics, structure-dynamics, electro-magnetics, audible noise, vibrations, surface-force density, manufacturing tolerances, electrical machines, electromagnetic energy converters.

1. INTRODUCTION

The coupled physics of a complete acoustic simulation – starting from the electromagnetic force excitation, computing the mechanical deformation of the electromagnetic device and concluding in the estimation of the radiated audible noise – is a multi-physics problem. The central part of the computational chain is the electromagnetic field simulation of which the surface-force density-waves are derived. These excite the stator of the machine resulting in vibrations. The periodical oscillation of the machines surface is decoupled and radiated as disturbing audible noise.
For the numerical structure-dynamical and acoustic tool, a number of software programs have to be coupled, trimming the interfaces in a reasonable manner. This affords a broad knowledge of the applied methods and their implementation. Therefore, an own tool box has been developed at the IEM compatible to all types of electromagnetic devices such as transformers, rotating electrical machines (DC-, AC-machines, switched reluctance machines), actuators, and others [1-4,31].
The structure of an entire acoustic multi-physics simulation-chain is shown in Fig. 1 [5]. In a first step a FEM-model of the electromagnetic device is simulated. A systematic, parameter-oriented model allows for a large number of geometry variations. Furthermore, various modes of operation can be considered. Hence, the effects of manufacturing tolerances can be taken into account as well as the designed geometry of the device [6]. The electromagnetic model provides the radial component of the surface-force density used as excitation for the structure-dynamical model. In the mechanical model various materials and geometries can be considered to analyse the vibration. Here, the variants of the electromagnetic model are considered as parameters. In the last step the audible noise of the multitude of variants is estimated and analysed with an acoustic Boundary-Element (BEM) model [7-10].

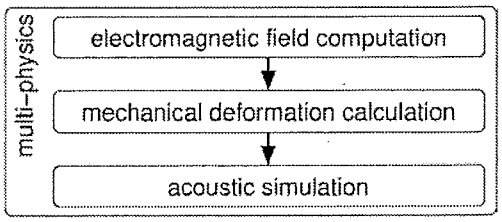

Fig. 1. Structure of the entire acoustic simulation-chain.

The acoustic simulation chain allows for the a-priori analysis of several machine variants at various modes of operation (e.g. operation on the grid or on a converter). An aimed systematic optimisation of the machine is performed based on this multi-physics problem. The resulting quantities are the sound pressure, the acoustic power of the sound pressure, the sound-particle velocity, and the sound intensity. In the following the three links of the simulation chain are discussed and examples show the efficiency of the applied tools.

2. ELECTROMAGNETIC FIELD COMPUTATION

As example for the electromagnetic field, problem an electrical machine is studied. For the solving of the problem the FEM is applied. The FEM can be applied for the simulation of 2-dimensional as well as 3-dimensional electromagnetic field problems. These can be static, time harmonic or transient. Therefore, the type of field problem has to be defined first. In the case of a long electrical machine the end effects can be neglected. If, furthermore, the flux paths are in the orthogonal plane to the rotor axis, a 2-dimensional FEM-model can be applied. For special 3-dimensional geometry effects such as skewing 2-dimensional models can be applied as well by interconnecting several 2-dimensional models [11-19]. In general all the other cases

require 3-dimensional models. The simulation of 2-dimensional FEM-models shows some significant advantages towards 3-dimensional models:

- 2-dimensional models are much smaller. Often the number of elements N_{el} is more than 10 times as small.
- The computation time of electromagnetic models is disproportionately high to N_{el}. Therefore, 2-dimensional models result in least computational costs.
- In general the discretisation of the geometry and in respect the accuracy increases since there are more elements in the cross section of the geometry than in the case of a 3-dimensional model. Using the same discretisation (element size) in the 3-dimensional model results in a non-reasonable N_{el}.

Therefore, 2-dimensional FEM-models should be applied whenever possible.

In this article an Induction Machine with squirrel-cage rotor (IM) and a Switched Reluctance Machine (SRM) are studied. Both electrical machines are simulated electromagnetically applying appropriate 2-dimensional FEM-models. The process is exemplarily described for the IM in the following.

The electromagnetic FEM-model of the IM, shown in Fig. 2 consists of the stator- and rotor laminations, the aluminium rotor bars, the copper winding of the stator, and the air gap. All other parts of the IM are not modelled not having any significant impact on the electromagnetic field in the IM. The boundaries of the IM at the shaft and the outer circumference are assigned with a Dirichlet boundary condition (tangential magnetic vector potential).

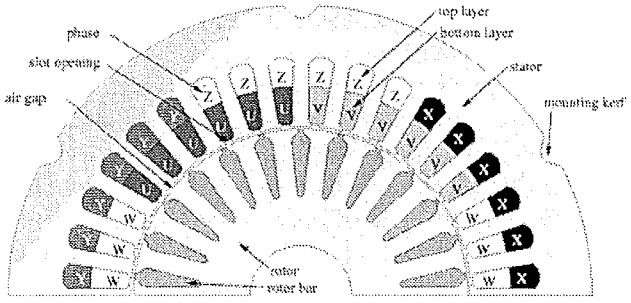

Fig. 2. Electromagnetic, 2-dimensional model of the IM.

The electromagnetic simulation is performed in the time domain. The IM-model is computed quasi-static for a fixed number of time steps N applying a transient solver [1,20,21]. At each time step the rotor is rotated depending on the rotor speed n and the time-step width Δt:

$$\Delta\alpha = \frac{180^\circ}{60^\circ} \cdot (n \cdot \Delta t) \,. \tag{1}$$

After rotating and re-meshing the air gap an appropriate stator current is assigned to the model and the flux-density distribution of the previous time step is taken into consideration for the right-hand side of the equation set. Hereby, the transient factor θ weights the previous solution [3]. Each of the models (one FEM-model per time step) represents a static electromagnetic field problem. From each of the field problems the magnetic vector potential results. Fig. 3 depicts the magnetic vector potential for one time step. The four magnetic poles of the machine can be seen easily. The flux-density distribution is given by

$$\vec{B} = \mathrm{rot}\,\vec{A} \,. \tag{2}$$

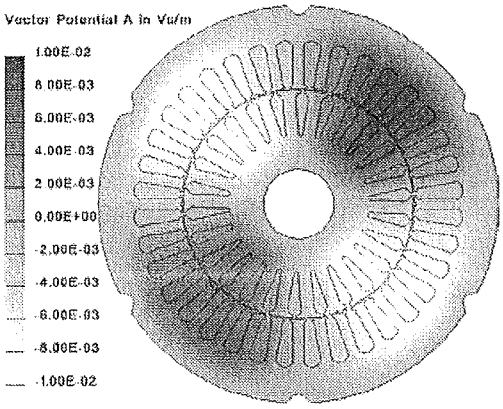

Fig. 3. Magnetic vector potential in the IM for one single time step.

The flux-density distribution in Fig. 4 shows that the highest values of B are reached in the tooth tips. Furthermore, the mounting kerfs on the outer circumference of the IM show some impact on the flux paths, constricting the flux and increasing the flux density slightly. Since the resulting values are below the saturation point of the iron lamination this has no significant effect on the motor's operational behaviour.

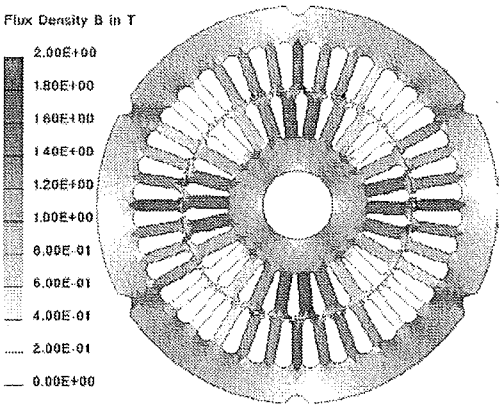

Fig. 4. Flux-density distribution in the IM for one single time step.

The number of simulation time steps N has to be chosen depending on the resolution of the spectrum of all regarded quantities. The preferred resolution of the spectrum of the surface-force density used as excitation for the structure-dynamical simulation has to be considered here. Both, the

cut-off frequency f_{co} of the spectrum and the resolution Δf depend on Δt and N:

$$\Delta f = \frac{1}{2 \cdot \Delta t \cdot N} \tag{3}$$

$$f_{co} = \frac{1}{2 \cdot \Delta t} . \tag{4}$$

From the flux-density distribution torque T, net force F, surface-force density σ, and other quantities are derived. For the acoustic simulation chain T and F are not of interest and therefore not regarded here. σ is calculated for each time step on the stator teeth using the Maxwell-stress tensor-method [22]. Next to σ, some specific electromagnetic devices such as transformers [23] afford the consideration of magnetostriction [33] or [24]. In regular rotating electrical machines σ predominates [25-28]. Therefore magnetostriction and Lorentz forces are neglected and only σ is taken into consideration further on.

Fig 5. shows the resulting force excitation of a 3-dimensional IM-model for one time step. The skewing of the rotor is reflected by the skewed force distribution on the teeth. The included zoom of one of the stator teeth shows, that at motor operation the highest magnitudes appear on the up-running edge of the teeth.

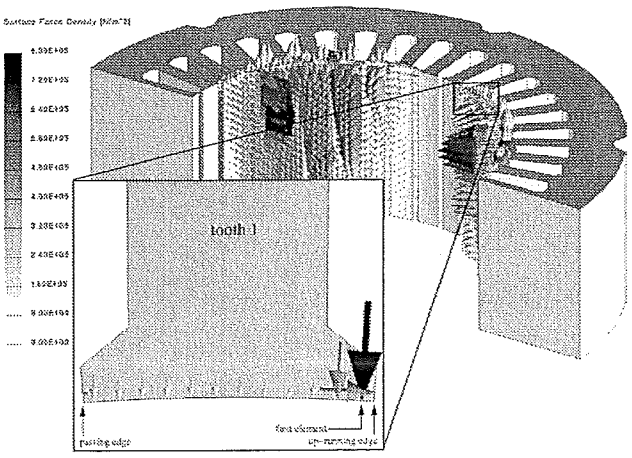

Fig. 5. Surface-force density-distribution on the stator teeth of the IM for one single time step.

The surface-force density of the marked first element of the tooth is transformed to the frequency domain and analysed. Fig. 6 depicts the resulting spectrum. The frequencies detected result from the fundamental and the harmonic air-gap field-components of the stator which interact with the fundamental and harmonic components of the rotor [25,26]. The harmonics depend on the point of operation defined by the speed n, the slip s, and the stator frequency f_1 as well as the winding arrangements of rotor and stator described by the number of pole pairs p, the stator and rotor slot numbers N_S and N_R, and the number of phases m. Table 1 collects these parameters for the studied IM and the regarded operation point.

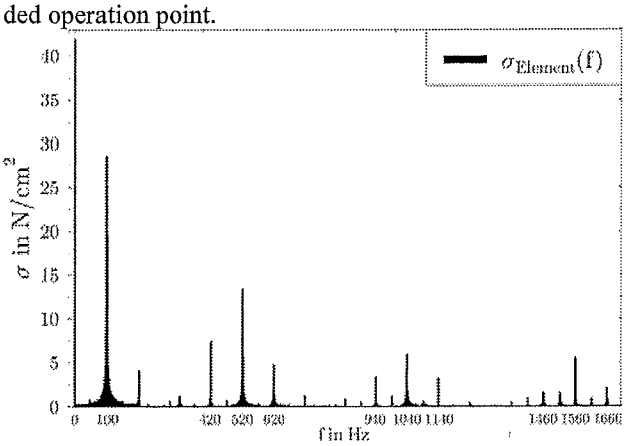

Fig. 6. Spectrum of the surface-force density of a single stator-tooth element.

Table 1. Parameters and point of operation of studied IM.

p	2	n	1200 rpm
N_S	36	f_1	48.96 Hz
N_R	26	s	0.183
m	3		

From these parameters the significant harmonic frequencies are calculated [25,26] listed in Table 2. These frequencies are considered in the following structure-dynamical simulation of the IM described in the next section.

Table 2. Significant harmonic frequencies.

$2f_1$	98 Hz	$N_R n + 2f_1$	422 Hz
$N_R n$	520 Hz	$N_R n - 2f_1$	618 Hz
$2 N_R n$	1040 Hz	$2 N_R n + 2f_1$	942 Hz
$N_S n$	720 Hz	$2 N_R n - 2f_1$	1138 Hz

3. STRUCTURE-DYNAMICAL COMPUTATION

After the electromagnetic simulation of an electrical machine, a structure-dynamical simulation is performed to determine the deformation or the oscillations. The surface-force density on the stator teeth, which is obtained from the electromagnetic simulation, is used as excitation. As in the electromagnetic case, the calculation of the periodic, mechanical deformation of electrical machines requires a numerical simulation. Due to the large numbers and complexity of its components, it is not possible to find an exact analytical solution. The structure-dynamical simulation is performed by means of FEM [1-3,31].

The deformation of the machine is represented by the displacement of the individual nodes of the mechanical FE-model [5,22,33]. Strain and deformation are related by:

$$\varepsilon = S \cdot \vec{u} \tag{5}$$

$$\text{with} \quad S = \begin{bmatrix} \frac{\partial}{\partial x} & 0 & 0 & \frac{\partial}{\partial y} & 0 & \frac{\partial}{\partial z} \\ 0 & \frac{\partial}{\partial y} & 0 & \frac{\partial}{\partial x} & \frac{\partial}{\partial z} & 0 \\ 0 & 0 & \frac{\partial}{\partial z} & 0 & \frac{\partial}{\partial y} & \frac{\partial}{\partial x} \end{bmatrix}^T \tag{6}$$

The correlation between the strain ε and the tension σ is given by Hooke's law. Neglecting initial strain and tension, this is expressed as

$$\sigma = H \cdot \varepsilon, \tag{7}$$

where H is Hooke's matrix. Its entries are defined by Young's modulus E and Poisson's ratio μ of the corresponding material. For the case of isotropic and homogenous bodies, it has the following form

$$H = \frac{E(1-\mu)}{(1-\mu)(1-2\mu)} \begin{bmatrix} 1 & \frac{\mu}{1-\mu} & \frac{\mu}{1-\mu} & 0 & 0 & 0 \\ \frac{\mu}{1-\mu} & 1 & \frac{\mu}{1-\mu} & 0 & 0 & 0 \\ \frac{\mu}{1-\mu} & \frac{\mu}{1-\mu} & 1 & 0 & 0 & 0 \\ 0 & 0 & 0 & \frac{1-2\mu}{2(1-\mu)} & 0 & 0 \\ 0 & 0 & 0 & 0 & \frac{1-2\mu}{2(1-\mu)} & 0 \\ 0 & 0 & 0 & 0 & 0 & \frac{1-2\mu}{2(1-\mu)} \end{bmatrix} \tag{8}$$

To decrease the computational effort to a reasonable measure, it is necessary to use equivalent materials in the simulation. For example, the laminated sheet stack of the stator is modelled as such an equivalent material with an anisotropic Hooke's matrix. The determination of its parameters relays on material identifying algorithms. One algorithm, which is used to obtain the material parameters of an electrical machine's stator is the Threshold-Accepting Method [32]. The potential energy of a body due to strain reads

$$\Pi_p = \int_\Omega \varepsilon^T H \varepsilon \, \mathrm{d}\Omega - \int_{\partial\Omega} \vec{u} \cdot \vec{\sigma}_s \varepsilon \, \mathrm{d}\, \partial\Omega, \tag{9}$$

where $\vec{\sigma}_s$ is the surface force density and Ω the volume of the body. The kinetic energy of an oscillating body reads

$$T = \int_\Omega \frac{\rho}{2} \cdot \dot{\vec{u}} \, \mathrm{d}\Omega, \tag{10}$$

with the mass density ρ of the body. The deformation-solver formulation is constructed using Hamilton's principle, i.e. minimising the Lagrange function

$$L = T - \Pi_p, \text{ by} \tag{11}$$

$$0 = \frac{d}{dt}\left(\frac{\partial L}{\partial \dot{\vec{u}}}\right) - \left(\frac{\partial L}{\partial \vec{u}}\right) + \left(\frac{\partial F}{\partial \dot{\vec{u}}}\right), \tag{12}$$

where F represents a damping function. After discretising, the following oscillation equation is obtained:

$$K \cdot D + C \cdot \dot{D} + M \cdot \ddot{D} = F. \tag{13}$$

K is the global stiffness matrix, D is the vector of the node deformation, C is the damping matrix and F is the excitation force [5]. Due to harmonic analysis, with

$$\dot{D} = \frac{dD}{dt} = j\omega D \tag{14}$$

equation (12) becomes

$$(K + j\omega C - \omega^2 M) \cdot D = F. \tag{15}$$

The complex surface force density F is transformed from the electromagnetic simulation to the mechanical model for each frequency, which is to be analysed. Then, the structure-dynamical simulation is performed. This can be done either by solving equation (15) directly for each individual

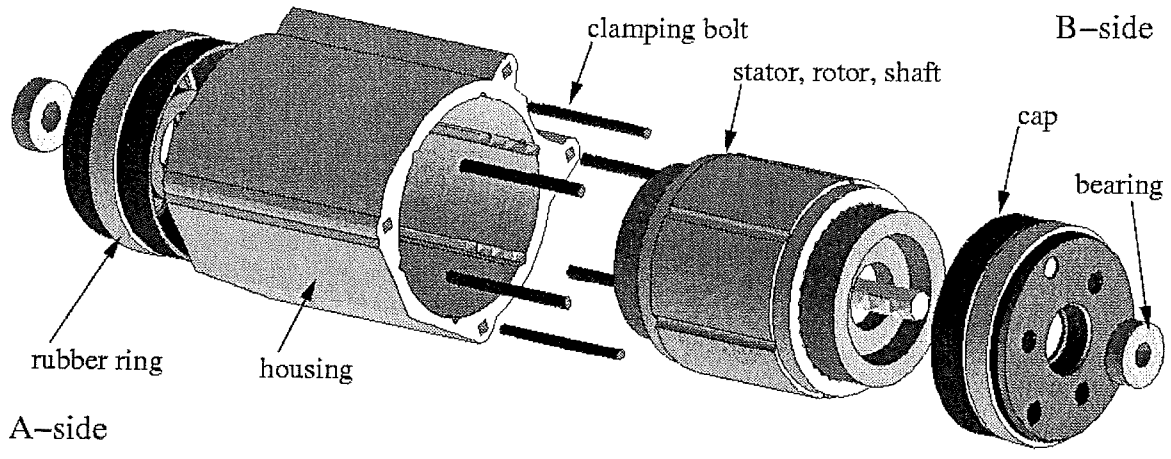

Fig. 7. Mechanical model (exploded view).

frequency separately, or by performing a modal analysis, i.e. finding the eigenvalues and eigenvectors of the corresponding eigenproblem, together with a subsequent modal super-position. The most suitable approach for solving the equation (15) depends on the application. For the structure-dynamical simulation of electrical machines, solving equation (15) for each frequency individually has been approved in practice [5].

The mechanical model (Fig. 7) consists of all components of the electrical machine. The surrounding air is not included in the model, since for the expected small deformations of maximally some micrometers, the influence of the air on the deformation of the solid body is negligible. Thus, the coupling between structure-dynamical and acoustic simulation can be considered a numerical weak coupling.

For the physical quantities of the deformation, there are different requirements concerning the detailing of the individual parts. The rotor, for example, may be represented as a solid cylinder. The housing, however, has to be modelled including much more details. As in the electromagnetic case, extensive experience is required to set up a correct structure-dynamical model [33].

The deformation of an electrical machine can be evaluated as follows:

- According to [25], certain modes of oscillation ensue, which depend on stator frequency, speed, numbers of slots, the number of pole pairs and the winding arrangement. The modes of oscillation allow conclusions concerning the mechanical strength. In addition, it is possible to determine the expected single tones. Small mode numbers r are considered to be critical. With an increasing mode number, the mechanical structure becomes stiffer, and hence can not be strongly deformed. A small deformation will enhance the acoustic behaviour. For example, mode numbers 0 and 1 are considered very critical, since they lead to large force excitations on to the bearings of the machine. Fig. 8 and 9 show, for example, a deformation of the stator of an induction machine, with mode number $r = 6$. As studies have shown, manufacturing failures and asymmetries have a large impact on the deformation modes, and therefore on the acoustic behaviour of electrical machines.

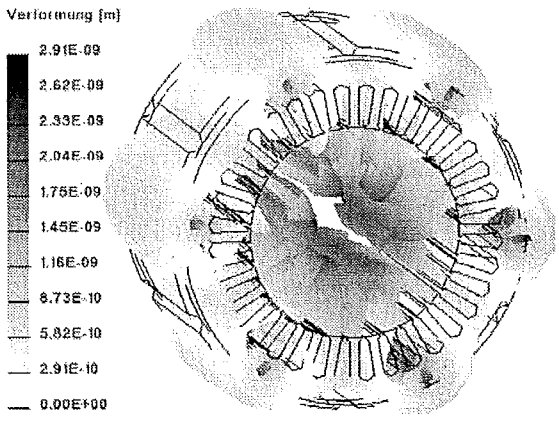

Fig. 8. Deformation of the stator at $f = 618$ Hz.

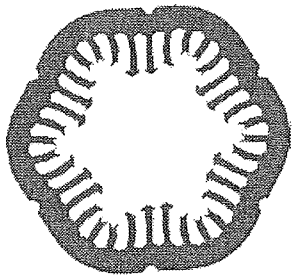

Fig. 9. Mode of deformation at $f = 618$ Hz.

- Alternatively, the body sound-level can be determined at fixed locations, which may be identical to measuring positions. The advantage of this method is its comparability, the disadvantage, however, is its locale scope. Therefore, the body sound-level does not provide conclusions about the behaviour of the complete structure.
- Oppose to the body sound-level, the body-sound index represents an integral quantity for the complete body. Using this index, it is possible to globally compare the deformation for different excitations.

Depending on the technical question, the right evaluation criterion is to be chosen.

Due to manufacturing tolerances, rotors of electrical machines are always supported eccentrically. For the machine design, the bearing is considered ideal, and centric support is assumed. Therefore, it is necessary to estimate the effects of the eccentric support. Fig. 10 shows the different rotationary eccentricities, which are due to manufacturing tolerances. In the centric case, the centres of the rotor, of the stator and of the rotation are located at the same position. For the eccentric cases, either the centres of the rotation and of the rotor (dynamical eccentricity) differ, or the centres of the rotation and of the stator differ (static eccentricity). Both eccentricities can occur together as combined static-dynamical eccentricity.

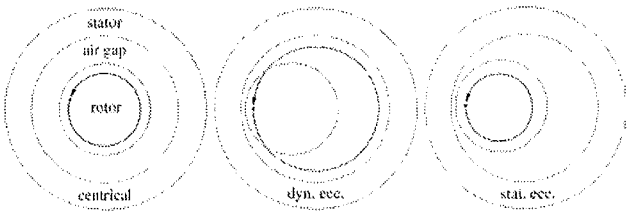

Fig. 10. Different rotationary eccentricities of the IM.

Fig. 11 shows the results for selected frequencies of an induction motor at different eccentricities of the rotor compared to the centric machine. It shows that for an eccentric machine an increase in deformation has to be expected. The static eccentricity leads to the largest body sound-level, and has to be regarded very critical [25]. It further shows that it can not be concluded from the excitation force density immediately to the oscillation of an electrical machine. For example, for $N_S\, n = 720$ Hz ($N_S = 36$) the larges deformation occurs, despite very small force magnitudes (Fig. 6).

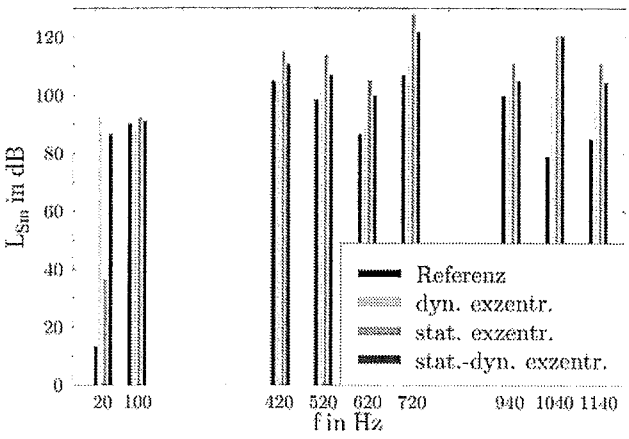

Fig. 11. Comparison of the body-sound index for eccentric models.

4. ACOUSTIC SIMUALTION

The acoustic noise radiated from electrical machines consists of three parts:

- The broad-band fan and ventilation noise (500 – 1000 Hz) results air turbulences generated by the rotating motor.
- Friction of the bearings of electrical machines is a further sound source, which generates single tones in the range larger than 3 kHz.
- Housing vibration excited by the electromagnetic field of electrical machines generates magnetic noise, which consists of single tones in the entire range of audibility.

The presented calculation method only discusses the noise radiation generated by the electromagnetic deformation (vibration).

For the acoustic simulation, the mechanical deformation of the machine is converted to the velocity. In principle, calculation of acoustic fields is possible with the FEM. However, for calculation of air-borne noise this method is unfavourable, since the entire calculation area has to be discretised. An alternative is offered by the BEM [5,29]. Here, only the surface of the area is discretised. Basic principle of the BEM is the solution of the Helmholtz differential equation

$$\Delta \underline{p} + k^2 \cdot \underline{p} = 0 \qquad (16)$$

with the sound pressure p and wave number $k = \omega/c$. Here, ω is the angular frequency and c the sound velocity. After further calculations the following equation system results:

$$H \cdot \underline{p} = G \cdot \underline{\vec{v}}\,. \qquad (17)$$

H and G are system matrices [5] and the velocity vector the excitation value. A numerical solution of equation (17) results in the sound pressure p. The used program contains the here presented procedure. For the use of this method a third, acoustic model of the electrical machine is needed (additional to the electromagnetic and mechanical model). This model only consists of the outer surface mesh, which represents the noise radiating area of the motor. The mechanical velocity is transferred to this acoustic mesh.

Since the BEM is applied, there is no solution for the air volume surrounding the machine. Therefore, sound pressure and sound particle velocity are evaluated on predetermined points or surfaces (Fig. 11 and 12). As further quantities acoustic power [30] and sound intensity of the machine are calculated. The results are available for discrete frequencies.

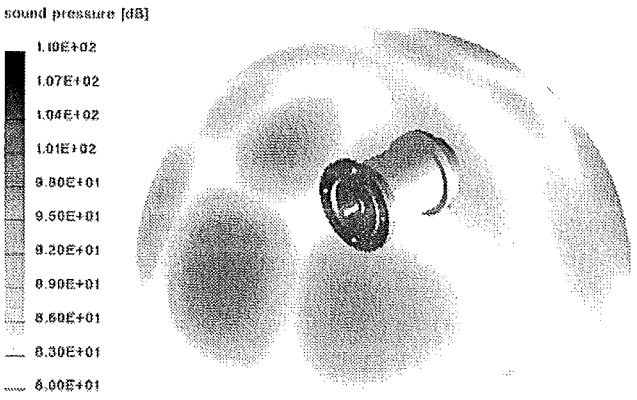

Fig. 11. Sound pressure distribution on the analysis sphere.

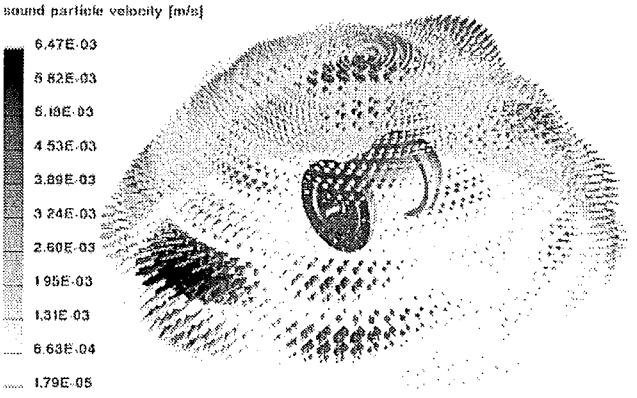

Fig. 12. Sound particle velocity field on the analysis sphere.

Here, evaluation of the acoustic simulation is presented for an SRM. Two current waveforms and two housing versions (aluminium and grey cast iron) are calculated for a selected operating condition. The simulated sound pressure and sound particle velocity are shown in Fig. 11. Direction of noise radiation and acoustic power can be determined by these quantities. At $f = 4400$ Hz the SRM radiates the most acoustic noise in axial direction.

Fig. 13 collects the results of both housing versions in the frequency range from 1200 to 3000 Hz. In the given example the noise radiation is also affected by the current waveform. Waveform 2 lowers the radiated noise. The aluminium housing produces more acoustic noise compared to the cast

iron housing. This is due to the higher material density of cast iron and the deviation of the Young's modulus. The results correspond to air-borne sound measurements.

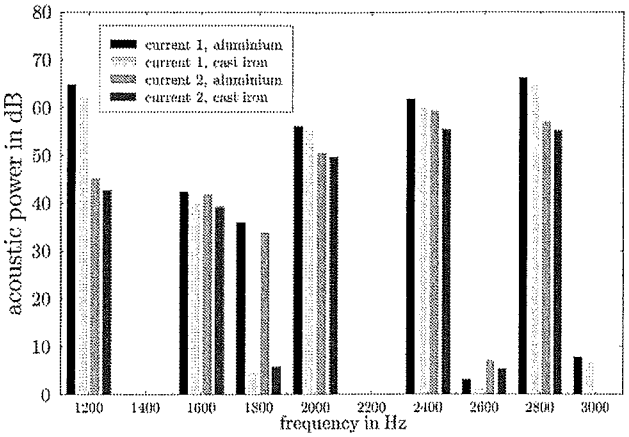

Fig. 13. Acoustic power for the studied operational condition of the SRM.

5. CONCLUSIONS

Numerical simulations allow for the consideration of the structure-dynamical and acoustic behaviour of an electrical machine a-priori during the phase of design. The proceeding of the numerical simulation is explained based on the considered machines (IM and SRM).

On the one hand, the simulated results show good accordance to measurement results, on the other hand the high optimisation potential concerning vibrations and noise of the analysed machines is presented. The presented methods and simulation tools allow the analysis and evaluation of every type of energy converter with respect to its electromagnetic, structure-dynamical and acoustic behaviour. By means of measurement devices it is also possible to verify the simulation results.

The analysis also provides the detection of manufacturing faults in electrical machines. Therefore, the numerical acoustic simulation is an essential tool for the design, validation and optimisation of electrical machines.

REFERENCES

[1] Arians, G., Bauer, T., Kaehler, C., Mai, W., Monzel, C., van Riesen, D., Schlensok, C., "Innovative modern object-oriented solver environment – iMOOSE", www.imoose.de, 2006.

[2] van Riesen, D., Monzel, C., Kaehler, C., Schlensok, C., Henneberger, G., "iMOOSE – an open-source environment for finite-element calculations", *IEEE Transactions on Magnetics* vol. 40, no. 2, pp 1390-1393, 2004.

[3] Zienkiewicz, O., Taylor, T., *The finite element method* vol. 1,2, McGraw-Hill Book Company, 1989.

[4] Kost, A., *Numerische Methoden in der Berechnung elektromagnetischer Felder* Springer-Verlag, 1994.

[5] Schlensok, C., van Riesen, D., Küest, T., Henneberger, G., "Acoustic Simulation of an Induction Machine with Squirrel-Cage Rotor", *COMPEL*, vol. 25 no. 2, pp. 475-486, 2006.

[6] Schlensok, C., Henneberger, G., "Comparison of static, dynamical and static-dynamical eccentricity in induction machines with squirrel cages using 2D-transient FEM", *COMPEL*, vol. 23 no. 3, pp. 1070-1079, 2004.

[7] Brebbia, C., *The boundary element method for engineers*, Pentech Press, London, 1978.

[8] Brebbia, C. (editor), *Topics in boundary element research*, Springer-Verlag, Berlin, 1984.

[9] Brebbia, C., Telles, J., Wrobel, L., *Boundary element techniques*, Springer-Verlag, Berlin, 1984.

[10] Hartmann, F., *Introduction to boundary elements method*, Springer-Verlag, Berlin, 1989.

[11] Boualem, B., Piriou, F., "Numerical models for rotor cage induction machines using Finite Element Method", *IEEE Transactions on Magnetics* vol. 34, no. 5, pp 3202-3205, 1998.

[12] Dziwniel, P., Boualem, B., Piriou, F., Ducreux, J.-P., Thomas, P., "Comparison between two approaches to model induction machines with skewed slots", *IEEE Transactions on Magnetics* vol. 36, no. 4, pp 1453-1457, 2000.

[13] Dziwniel, P., Piriou, F., Ducreux, J.-P., Thomas, P., "A time-stepped 2D-3D finite element method for induction motors with skewed slots modelling", *IEEE Transactions on Magnetics* vol. 35, no. 3, pp 1262-1265, 1999.

[14] Piriou, F., Razek, A., "A model for coupled magnetic-electric circuits in electric machines with skewed slots", *IEEE Transactions on Magnetics* vol. 26, no. 2, pp 1096-1100, 1990.

[15] Williamson. S., Lim, L. H., Smith, C., "Transient analysis of cage-induction motors using Finite Elements", *IEEE Transactions on Magnetics* vol. 26, no. 2, pp 941-944, 1990.

[16] Williamson. S., Flack, T. J., Volschenk, A. F., "Representation of skew in time-stepped two-dimensional finite-element models of electrical machines", *IEEE Transactions on Magnetics* vol. 31, no. 5, pp 1009-1015, 1995.

[17] Gyselinck, J. J. C., Vandevelde, L., Melkebeek, J.A. A., "Multi-Slice FE Modelling of electrical machines with skewed slots – the skew discretization error", *IEEE Transactions on Magnetics* vol. 37, no. 5, pp 3233-3237, 2001.

[18] Ho, S. L., Fu, W. N., "A comprehensive approach to the solution of direct-coupled multi slice model of skewed rotor induction motors using time-stepping eddy-current Finite Element Method", *IEEE Transactions on Magnetics* vol. 33, no. 3, pp 2265-2273, 1997.

[19] de Oliveira, A. M., Antunes, P., Kuo-Peng, P., Sadowski, N., Dular, P., "Electrical machine analysis considering field – circuit – movement and skewing effects", *COMPEL*, vol. 23 no. 3, pp. 1080-1091, 2004.

[20] Albertz, D., Henneberger, G., "On the use of the new edge based A-A, T formulation for the calculation of time-harmonic, stationary and transient eddy current field problems", *IEEE Transactions on Magnetics* vol. 36, no. 4, pp 818-822, July 2000.

[21] De Gersem, H., Gyselinck, J. J. C., Dular, P., Hameyer, K., Weiland, T., "Comparison of sliding-surface and moving-band techniques in frequency-domain finite-element models of rotating machines", *COMPEL*, vol. 23 no. 3, pp. 1007-1014, 2004.

[22] Ramesohl, I., Henneberger, G., Küppers, S., Hadrys, W., "Three dimensional calculation of magnetic forces and displacements of a claw-pole generator", *IEEE Transactions on Magnetics* vol. 32, no. 3, pp 1685-1688, 1996.

[23] Kubiak, W., Witczak, P., "Magnetostriction vibration of transformer core", *3rd International Seminar on Vibrations and Acoustic Noise of Electric Machinery, VANEM*, Lodz, Poland, pp 71-75, 2002.

[24] Bauer, T., Henneberger, G., "Three-dimensional calculation and optimization of the acoustic field of an induction furnace caused by electromagnetic forces", *IEEE Transactions on Magnetics* vol. 35, no. 3, pp 1598-1601, 1999.

[25] Jordan, H., *Geräuscharme Elektromotoren* Verlag W. Giradet, 1950.

[26] Timar, P. L., *Noise and Vibration of electrical machines* Elsevier, Oxford, 1989.

[27] Witczak, P., Kubiak, W., Mlotkowski, A., Szulakowski, J., "Calculations of local magnetic forces in electric machinery", *1st International Seminar on Vibrations and Acoustic Noise of Electric Machinery, VANEM*, Bethune, Belgium, pp 57-61, 1998.

[28] Belmans, R., Hameyer, K., "Impact of inverter supply and numerical calculation techniques in audible noise problems", *1st International Seminar on Vibrations and Acoustic Noise of Electric Machinery, VANEM*, Bethune, Belgium, pp 9-23, 2002.

[29] Mai, W., Henneberger, G., "Object-oriented design of finite element calculations with respect to coupled problems", *IEEE Transactions on Magnetics* vol. 36, no. 4, pp 1677-1681, 2000.

[30] Kollmann, F. G., *Maschinenakustik* Springer-Verlag, Berlin, 2000.

[31] Bathe, K.-J., *Finite Elemente Methoden*, Springer-Verlag, 1986.

[32] Ramesohl, I., Henneberger, G., "Automatic structural material identification of electrical machines using the threshold accepting procedure", *11th Conference on the Computation of Electromagnetic Fields, Compumag*, Rio de Janeiro, Brazil, 1997.

[33] Delaere, K., *Computational and experimental analysis of electric machine vibrations caused by magnetic forces and magnetostriction*, PHD-Thesis, Katholieke Uni Leuven, 2002.